Q. J. R. Meteorol. Soc. (2003), **129**, pp. 1469–1490 doi: 10.1256/qj.01.91

Numerical diagnosis of a small, quasi-tropical cyclone over the western Mediterranean: Dynamical vs. boundary factors

By V. HOMAR[1]*, R. ROMERO[1], D. J. STENSRUD[2], C. RAMIS[1] and S. ALONSO[1,3]

[1]*Universitat de les Illes Balears, Spain*
[2]*NOAA/National Severe Storms Laboratory, USA*
[3]*IMEDEA, UIB-CSIC, Spain*

(Received 29 May 2001; revised 19 April 2002)

SUMMARY

A small, quasi-tropical cyclone occurred on 12 September 1996 over the western Mediterranean. Intense convective activity over the region during this period also produced a tornado outbreak in the Balearic Islands and torrential precipitation over eastern mainland Spain.

Mesoscale model runs properly simulate the cyclone formation and show convection and heavy precipitation following the cyclone trajectory during its eastward progression. A sensitivity study examining the upper-level dynamic forcing, latent- and sensible-heat fluxes from the sea, and orography is conducted. A potential-vorticity (PV) inversion technique is used to reduce the amplitude of the upper-level trough in the model initial conditions. The results show that neither the orography nor the sensible-heat flux from the sea play a significant role during this particular cyclone development. Conversely, both the latent-heat flux and the upper-level trough are shown to be crucial for low-level cyclogenesis. Features common to hurricane-like polar lows are found for the cyclone, and an analysis of the precise role of the upper-level structures and the convective development is conducted.

A factor-separation technique is used to determine the individual effects of the aforementioned factors, as well as their interaction. At the first stage of the cyclogenesis, the upper-level PV anomaly enhanced the low-level circulation of the synoptic-scale low and enhanced the latent-heat flux from the sea. During its mature stage, the circulation associated with the small-scale cyclone enhanced the latent-heat flux from the sea, thereby helping to maintain the development of deep convection, and inducing further cyclone deepening by diabatic heating. This scenario has many similarities with the air–sea interaction instability mechanism. Thus, the joint action of the upper-level anomaly, as a spin-up agent, and the latent-heat flux, as a sustainer of convection, emerges as the primary factor for the genesis and evolution of the small quasi-tropical cyclone.

KEYWORDS: Air–sea interaction Cyclogenesis Factor separation Potential-vorticity inversion

1. INTRODUCTION

On 11 and 12 September 1996 severe weather occurred over the western Mediterranean (see Fig. 1 for a geographical reference). Heavy precipitation was observed at Valencia, six tornadoes developed over the Balearics, and a small, deep, warm-core cyclone formed offshore the Valencian coast and moved eastwards during 12 September, producing strong winds in the Balearic Islands. This cyclone was approximately 150 km in diameter and produced an observed pressure drop at Palma de Mallorca of 11 hPa in just a few hours (Homar *et al.* 2001).

The western Mediterranean is well known as an important cyclogenetic area (e.g. Petterssen 1956; Alpert *et al.* 1990; Campins *et al.* 2000). However, small-scale cyclones having diameters of only a few tens of kilometres are uncommon. Reale and Atlas (2001) highlighted the anomalous characteristics of two small-scale cyclones that occurred one month later than that of the present study. They described several tropical-like features associated with the cyclones, and show the importance of the upper-level forcing to the low-level cyclogenesis. Pytharoulis *et al.* (1999) studied a hurricane-like cyclone that developed over south-eastern Italy, documented the presence of a warm core, and pointed out the crucial role played by the surface fluxes of heat and moisture on the cyclogenesis in which the influences of the sensible- and latent-heat fluxes from the sea were comparable. Alpert *et al.* (1999) documented a shallow cyclone that occurred

* Corresponding author: Departament de Física, Universitat de les Illes Balears, 07071 Palma de Mallorca, Spain. e-mail: victor.homar@uib.es

over the Gulf of Antalya in the eastern Mediterranean, mainly generated by orographic influence, but sustained by the latent-heat flux from the sea. Another small cyclone, that produced tropical storm intensity winds, formed to the south of Italy within a decaying synoptic low on 26 January 1982 (Ernst and Matson 1983).

Similar small-scale cyclones, called polar lows, are observed over the high-latitude oceans (Rasmussen 1985; Bresch *et al.* 1977). Businger and Reed (1989) present a 'cold-low' type of polar low which occurs embedded in synoptic-scale cold-core lows. These are preceded by deep convection that is maintained throughout the mature stage of the low. In addition, these lows have a warm core, generated from diabatic processes, that contributes to further intensification through the generation of low-level potential vorticity (PV). Businger and Reed (1989) highlight the hurricane-like character of these lows and suggest that diabatic destabilization is a mechanism for sustaining their strength. Bresch *et al.* (1997) present a numerical study of a polar low with a warm core that was influenced by deep convection. They note that substantial modification of the boundary layer is needed both before and during the polar-low development, and remark on the essential role of the latent heating in convective clouds. Referring to the role of the baroclinic instability, they conclude that baroclinic growth is able to proceed at the observed scales only within an environment of reduced stability at low levels, following the results of Staley and Gall (1977). For the Mediterranean basin in particular, Rasmussen and Zick (1987) discuss the polar-low-like features of a hurricane-like development in the Mediterranean which developed in the central part of a synoptic-scale surface low and after the triggering of deep convection.

Air–sea interaction instability was proposed by Emanuel (1986) as a tropical cyclone model which accounted for the importance of the evolving oceanic energy budget and was not based on a pre-existing conditionally unstable environment. Satisfactory predictions about the maintenance of a 'Carnot'-like heat engine are obtained from the air–sea interaction, but an initial spin-up of the cyclone, typically from organized convection, is necessary. Emanuel and Rotunno (1989) presented a study of a polar low in the Barents Sea north of Norway using an air–sea interaction model, which elucidated a number of thermodynamic similarities between tropical hurricanes and polar lows. They conclude that *disturbances of substantial amplitude are apparently necessary to initiate cyclone intensification by air–sea interaction.*

The high orographic ranges that surround the western Mediterranean Sea are known to favour convective activity and, in general, severe weather. Romero *et al.* (1997) and Doswell III *et al.* (1998), among others, describe several heavy-precipitation events over this region and show the crucial effect of the orography. Upslope flow forcing, or certain mesoscale modifications to the low-level circulation, is usually crucial for the triggering of convection. Furthermore, the warming and moistening of the boundary layer through the sensible- and latent-heat fluxes from the usually warm sea is also an efficient mechanism for convective destabilization and further production of heavy precipitation. In particular, the effect of moistening the low levels is two-fold: it favours the conditional destabilization of the boundary layer, facilitating the release of convection, and it allows a continuous replenishment of the buoyant energy, favouring the maintenance of convection.

The small cyclone presented here developed offshore the Valencian coast during the early morning of 12 September 1996. It moved eastwards and produced strong gusty winds over the Balearic Islands during the day. Homar *et al.* (2001) presented a diagnosis of the tornado outbreak that began late on 11 September and continued into early 12 September over the Balearic Islands. The role of the warm advection at low levels, induced by a broad synoptic-scale low over the western Mediterranean Sea, and

TABLE 1. CONFIGURATION OF THE NUMERICAL EXPERIMENTS PERFORMED

Experiment	Orography	Sensible-heat flux	Latent-heat release	Latent-heat flux	Potential-vorticity anomaly
EXP11	1	1	1	1	1
EXPNORO	0	1	1	1	1
EXPNSHF	1	0	1	1	1
EXPNLHR	1	1	0	1	1
EXP01	1	1	1	0	1
EXP10	1	1	1	1	0
EXP00	1	1	1	0	0

1 indicates the factor is activated during the simulation and 0 that it is not.

the presence of a cold cut-off low at mid and high levels were highlighted as the main synoptic-scale ingredients for the development of severe convection. They identified the small, quasi-tropical cyclone and presumed the influence of its associated circulation on the occurrence of some tornadic thunderstorms through the generation of a north-eastwards progressing surface convergence line between the quasi-tropical cyclone and the synoptic low.

In this study, to evaluate the influence of the mid-to-upper-level tropospheric cut-off low, its corresponding PV structure is identified. A PV-inversion technique following Davis and Emanuel (1991) is applied to obtain the balanced mass and wind fields associated with the PV anomaly. Studies by Bleck (1990) and Huo *et al.* (1999), among others, clearly show the advantages of synthesizing the classical vorticity and temperature advection forcings into a single field diagnostic when studying cyclogenesis due to baroclinic instability. In order to evaluate the role of the upper-level dynamic forcing, and its interaction with sea surface evaporation, on the genesis and evolution of the cyclone, the factor-separation technique of Stein and Alpert (1993) is used. The application of the PV-inversion technique allows one to define, in a practical way, a dynamical structure as a physical factor in the factor-separation technique (Tsidulko and Alpert 2001). In particular, the intensity of the upper-level cut-off low can be considered as a physical factor and its role in the cyclogenesis evaluated.

This study quantitatively analyses the effects of the aforementioned upper-level cut-off low, the orography, and the sensible-heat flux and evaporation from the sea, on the quasi-tropical cyclone formation. The relative importance of each of the factors, and their interactions, to the genesis and evolution of the system is determined by means of numerical simulations. Section 2 presents the characteristics of the numerical experiments, as well as the results obtained from the control run. The control run is used to introduce briefly the meteorological situation in which the episode occurred. The role of the upper-level dynamics, and evaporation from the sea, on the genesis and evolution of the cyclone is discussed in section 3. Final discussion and conclusions are presented in section 4.

2. CONTROL RUN

(*a*) *Experimental configuration*

A set of numerical simulations (Table 1) was performed in order to determine the mechanisms responsible for the extraordinary cyclonic development of 12 September 1996 over the western Mediterranean. The non-hydrostatic version of the Fifth generation Pennsylvania State University–National Center for Atmospheric Research (NCAR) Mesoscale Model MM5V2 (Dudhia 1993; Grell *et al.* 1995) was used. Global analyses from the National Centers for Environmental Prediction (NCEP), available at 0000 and

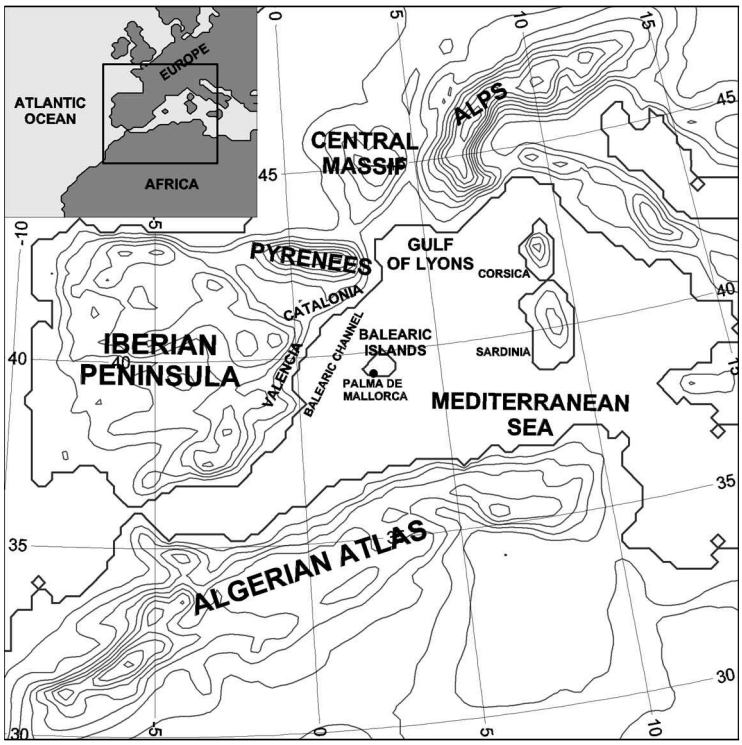

Figure 1. The western Mediterranean area including the locations referred to in the text. The large map shows the area and topography used for the inner domain in the numerical simulations. The top-left insert shows the area covered by the coarser domain.

1200 UTC, were considered as a first guess for a successive-correction objective analysis (Benjamin and Seaman 1985), which is used to include surface and upper-air observations to the model initial and boundary conditions. Since the cyclone formed during the first hours of 12 September 1996, a simulation starting at 1200 UTC 11 September, and extending out to 36 h, was chosen in order to account for the spin-up time of the model. Two domains are used to obtain higher resolution over the area of interest without excessive computational expense (Fig. 1). The coarse 82 × 82 grid-point domain, with 60 km resolution using a Lambert conformal projection, covers most of Europe, north Africa and part of the Atlantic Ocean. A two-way nesting strategy is used to interact with the nested 109 × 109 grid-point domain of 20 km resolution. This grid covers the western Mediterranean area, including the Iberian Peninsula and most of France. In the vertical, 32 terrain-following σ levels were used with enhanced resolution in the lower troposphere. Time steps for the fine and coarse grids are 60 and 180 s, respectively. Of particular interest is the formulation of the diabatic heating produced by latent-heat release in the convective systems developed during the simulation. The Kain and Fritsch (1990) convective parametrization scheme was used for both domains. For the resolved-scale moist processes, the microphysics scheme of Tao and Simpson (1993), based on the Lin *et al.* (1983) mixed-phase scheme, was used in both domains for consistency. It includes cloud and rain water, ice phase, and an equation for prediction of graupel. For boundary-layer processes, a modified version of the Hong and Pan (1996) planetary boundary-layer parametrization scheme was used, which uses a countergradient equation and an assumed k-profile for diffusion processes. Tests with the improved

surface flux calculations of Pagowski and Moore (2001) show very similar results to those presented in later sections. A five-layer soil model predicts land temperature using a vertical-diffusion equation. The sea surface temperatures (SSTs) are kept constant during the simulation and are obtained from the NCEP weekly database. The radiation calculations account for long- and short-wave interactions and include cloud–radiative effects.

(*b*) *Model validation*

A validation of the control run EXP11 is necessary to evaluate the ability of the model to reproduce this episode. The model simulates accurately the development and evolution of the small cyclone, though a consistent southward offset in its trajectory is found. While the actual cyclone formed and evolved about 100 km northwards of that obtained in the control run, its eastern progression and development are well simulated (Fig. 2(a)). Despite its small size, the model correctly develops the cyclone and also captures its depression intensity (Fig. 2(b)). The time series of the observed and simulated sea-level pressure exhibit a remarkable agreement during the entire simulation period, likely reflecting the correct simulation of the cyclone shape close to its centre.

A reasonable prediction of the precipitation field is needed before the model simulation can be used as a basis for sensitivity tests. A comparison of the 24 h accumulated precipitation at 0700 UTC 12 September, recorded by rain-gauges, and the accumulated precipitation obtained with the model at 0600 UTC indicates good agreement between both fields (Fig. 3). The small, isolated rainfall nucleus located over Valencia is properly reproduced by the model, though lower amounts are simulated. Significant precipitation over the sea can be deduced from the radar images shown by Homar *et al.* (2001), and correspond to the western rainfall-pattern elongation simulated over the Balearic channel in Fig. 3(b). In spite of the reasonably good fitting of the simulated precipitation with the observations near eastern Spain, convection identifiable on the satellite images to the north of the basin (from the Catalonia region to Corsica and Sardinia) is missed by the model (Fig. 21 of Homar *et al.* (2001)). This error likely does not affect the simulation of the small cyclone, and therefore the run is considered valid for further diagnosis and the application of numerical analysis techniques.

(*c*) *Diagnosis*

The synoptic situation as simulated by the model on 0000 UTC 12 September, less than 6 h before the cyclone formation, is characterized at low levels (Fig. 4(a)) by a large low-pressure system covering most of the western Mediterranean Sea and occurring within a strong baroclinic zone. An intense cold front from the Atlantic, with negative advection behind it, is identifiable to its south; a warm front accompanying the low is seen as an elongated warm-air tongue stretching eastward into the Mediterranean. Warm advection together with high moisture content is present in the lower tropospheric layers over the Balearic channel region. In addition, the synoptic-scale low produces north-easterly winds over eastern Spain. North-easterly trajectories were described to be crucial for the development of torrential rainfall events in the Valencia region (Romero *et al.* 2000). The interaction with local topography (Homar *et al.* 1999), the efficiency for moistening the boundary layer (Ramis *et al.* 1998), and the helicity generated in combination with the upper-level south-southwesterly flow (Tudurí and Ramis 1997) are important mechanisms for heavy rainfall production in the area. At 500 hPa (Fig. 4(b)), a cold cut-off low is identifiable, with a vorticity advection maximum to the south of the Iberian Peninsula. At 300 hPa (Fig. 5(a)), a PV nucleus of more than 3 PV units

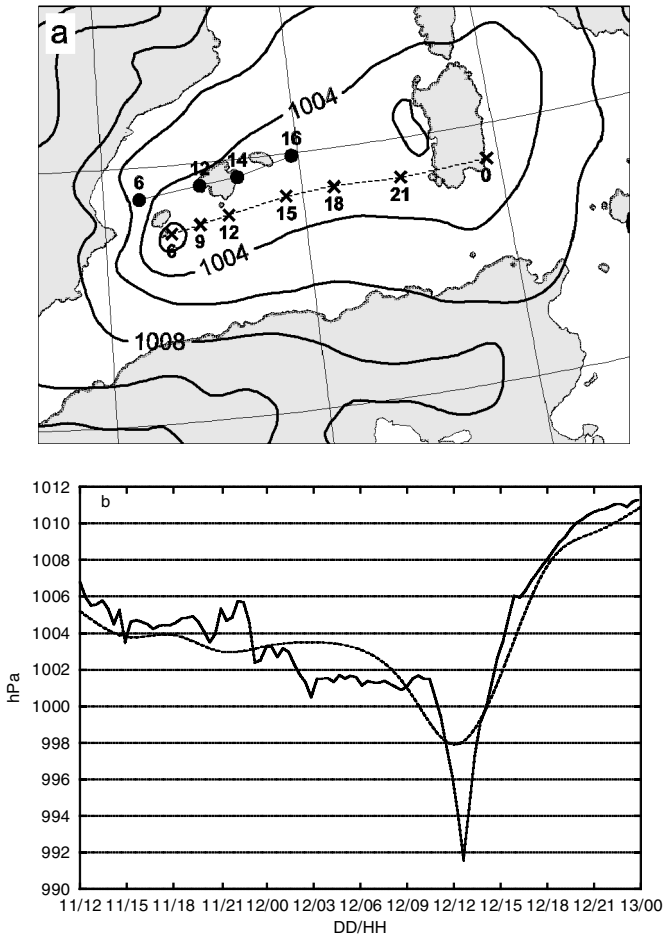

Figure 2. (a) Sea-level pressure (hPa) at 0600 UTC 12 September 1996 for EXP11 (see text). Crosses and adjacent numbers indicate the position and time (UTC) of the cyclone centre as simulated by EXP11. Dots and adjacent numbers indicate the location and time (UTC) of the cyclone centre as diagnosed from satellite and radar images. (b) Pressure (hPa) as recorded at Palma de Mallorca (full line) and as simulated by the model at the closest grid point to Palma de Mallorca of the simulated cyclone-centre trajectory (dotted line).

(1 PVU $= 10^{-6}$ K m^{2}s^{-1}kg^{-1}) was present south of the Iberian Peninsula at 0600 UTC 12 September. This upper-level PV feature moved north-eastwards over the western Mediterranean Sea during the following hours (Fig. 5(b)). Simultaneous with this shift of the upper-level PV nucleus, heavy precipitation occurred over eastern Spain, and the small-scale cyclone developed a closed circulation on the cold side of the synoptic-scale low, as indicated by both observations and the model.

At 0300 UTC (Fig. 6(a)), an area of intense evaporation associated with surface winds stronger than 10 m s^{-1} is present over the Balearic channel, and heavy precipitation of more than 60 mm in 3 h is produced. A westward elongation of the isobars is seen from the Balearics towards the eastern coast of Spain. Three hours later, at 0600 UTC (Fig. 6(b)), the cyclone has developed, resulting in both increased surface winds and increased latent-heat flux to the west of the cyclone centre. Heavy precipitation still is produced to the west and north-west of the cyclone, where warm and moist low-level air is advected towards the Spanish coast. Over the following hours (Fig. 6(c)), the cyclone

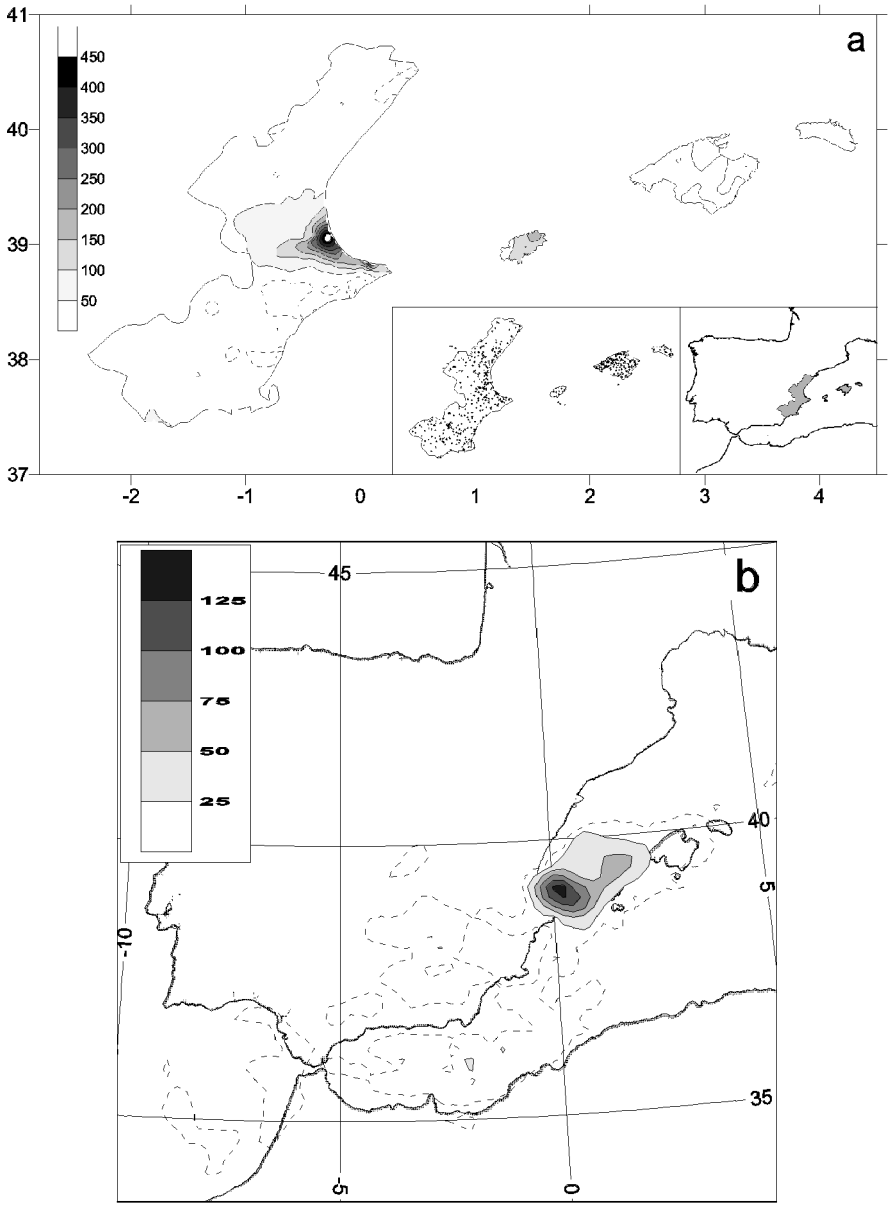

Figure 3. (a) Analysis of the 24 h accumulated rain-gauge precipitation (mm) at Valencia and the Balearics at 0700 UTC 12 September 1996. Inserted bottom panels show the distribution of the 646 rain-gauge stations used to perform the analysis and the location of the represented area in reference to the domain shown in (b). (b) Model forecast accumulated precipitation at 0600 UTC 12 September 1996. The dashed line depicts the 10 mm isohyet.

moved to the east and kept feeding the western convective systems with moist warm air through intense latent-heat flux from the sea and warm advection to its north. This close linkage between the cyclone and the convective systems is a characteristic feature of the 'cold-low' polar lows presented by Businger and Reed (1989). In addition, the intense latent-heat flux from the sea is an indication of possible air–sea interaction instability, which likely was triggered by the upper-level forcing in this case.

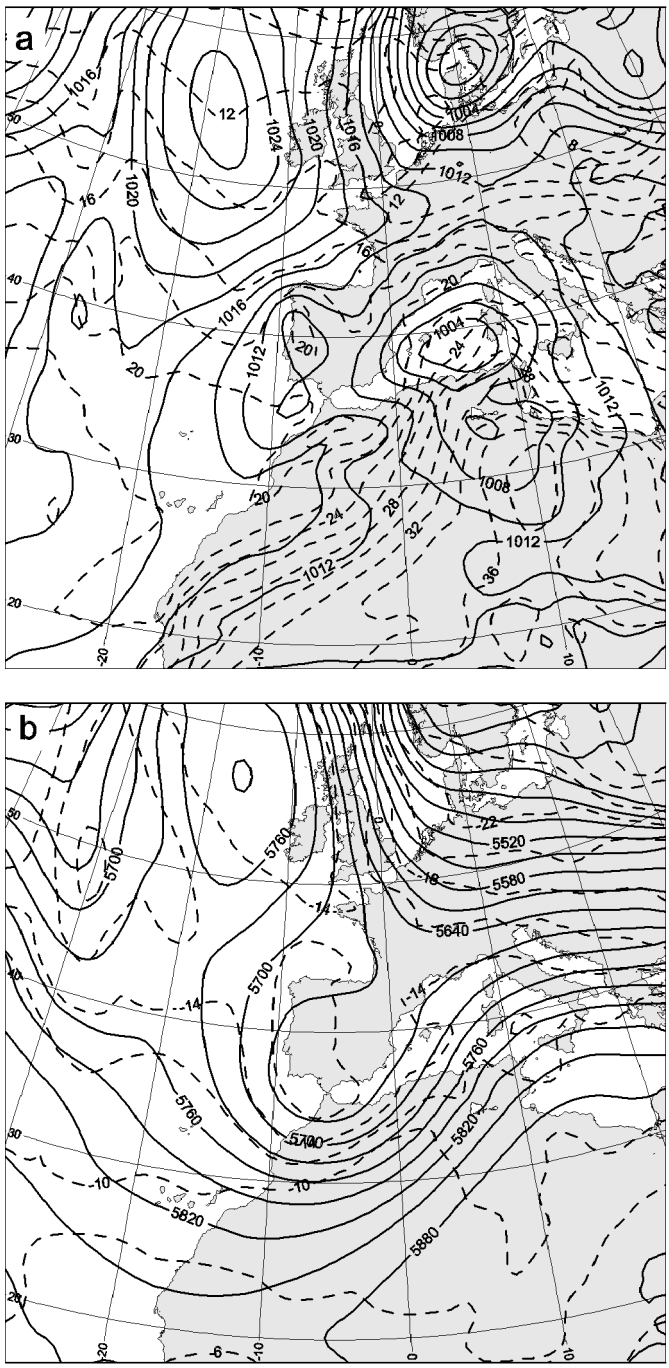

Figure 4. (a) Sea-level pressure (hPa, full lines) and temperature (°C, dotted lines) at 1000 hPa, and (b) geopotential height (gpm, full lines) and temperature at 500 hPa on 0000 UTC 12 September 1996, as simulated by the model.

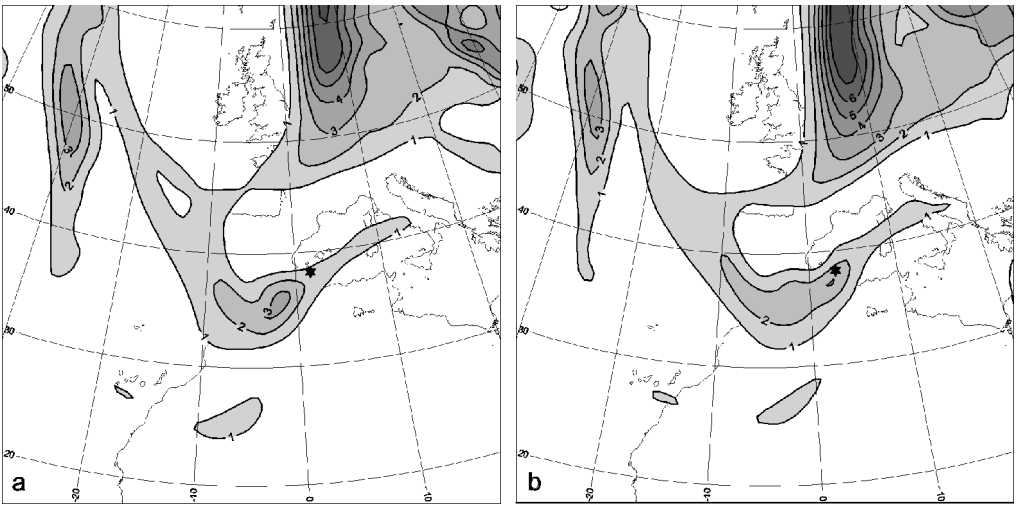

Figure 5. Potential vorticity (PV units) at 300 hPa at (a) 0600 UTC and (b) 1200 UTC 12 September 1996, as simulated by the model. Stars indicate the location of the simulated cyclone centre.

A vertical cross-section through the simulated cyclone at 1200 UTC 12 September shows a deep column of PV values higher than 1 PVU associated with the cyclonic circulation, together with a strong upward flow that indicates the presence of resolvable-scale convection to the west of the cyclone (Fig. 7). The cooperation of the parametrized and resolvable-scale convection in mesoscale simulations of convective systems has already been documented and discussed by Kain and Fritsch (1997). A vertical cross-section of equivalent potential temperature (EPT) across the surface cyclone centre (Fig. 8) also shows the convective activity over the cyclone centre. Additionally, the vertical distribution of EPT shows convective instability to the east of the cyclone centre and a convectively stable environment to its west. This suggests that the latent-heat release from convection is a primary reason for the intense cyclogenesis. It further appears that the diabatic warming derived from convection generated the deep PV anomaly column (Fig. 7).

Thus, the relationship between moist processes and the formation of the small cyclone also emerges from this simulation since convective development over the Balearic channel precedes the cyclone formation and follows its movement during its mature evolution. This suggests that air–sea interaction is playing a role in this hurricane-like development: the cyclonic circulation enhances the surface latent-heat flux, which leads to a vigorous latent-heat release from the convection, strengthening the cyclone and further enhancing the surface fluxes as the low-level winds increase.

3. CYCLOGENESIS SENSITIVITY

The diagnosis of the control run suggests that the pre-existing low-level circulation associated with the synoptic-scale low over the western Mediterranean may have been important to the development of convection and the first stages of the quasi-tropical cyclone genesis. The synoptic flow interacted with the orography surrounding the western Mediterranean basin, and in particular the Atlas mountain range, which could have had a significant influence on the cyclone evolution. The dynamic forcing associated with the upper-level cut-off low also may be important for the generation and

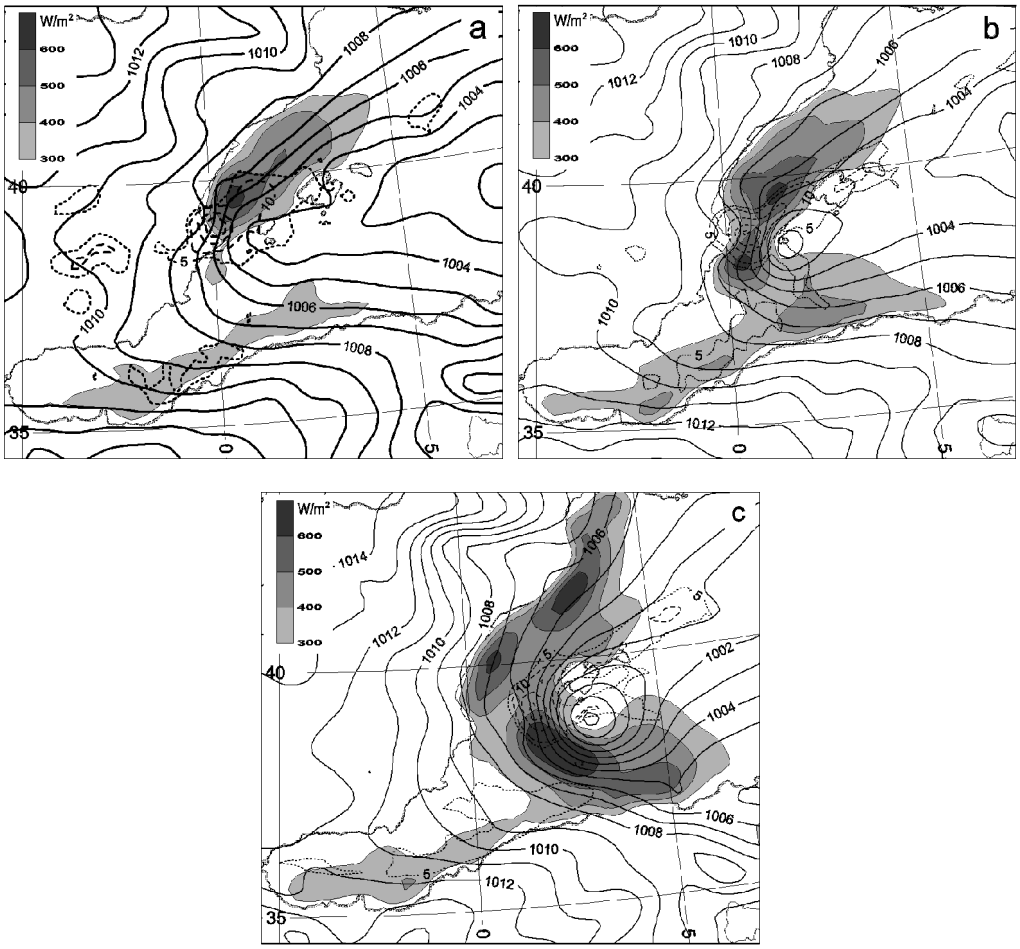

Figure 6. Sea-level pressure (hPa, full line), 3 h accumulated precipitation (mm, interval of 20 mm, dashed line) and latent-heat flux (W m^{-2}, shaded) as simulated by the model at: (a) 0300 UTC, (b) 0600 UTC and (c) 1200 UTC 12 September 1996. The dotted line depicts the 5 mm isohyet.

intensification of the cyclone and modifications to the mesoscale flow fields. In addition, evaporation from the Mediterranean Sea is a key mechanism for the moistening of the boundary layer. It is presumed that air–sea interaction instability is occurring, with latent- and sensible-heat fluxes being key energy sources for the ongoing diabatic heating associated with convection. To evaluate these proposed mechanisms, numerical experiments are performed to assess quantitatively the role of the orography, latent- and sensible-heat fluxes, and upper-level disturbance intensity on the genesis and evolution of the quasi-tropical cyclone.

Table 1 contains a schematic description of the five additional simulations performed for this evaluation. To confirm the air–sea interaction ideas that emerged from the diagnosis, an additional simulation (hereafter, EXPNLHR) with no latent-heat release from convection is performed (no convective parametrization and the elimination of the diabatic heating from condensation in the microphysics parametrization). The experiment with flat orography (hereafter, EXPNORO) contains no terrain-induced effects

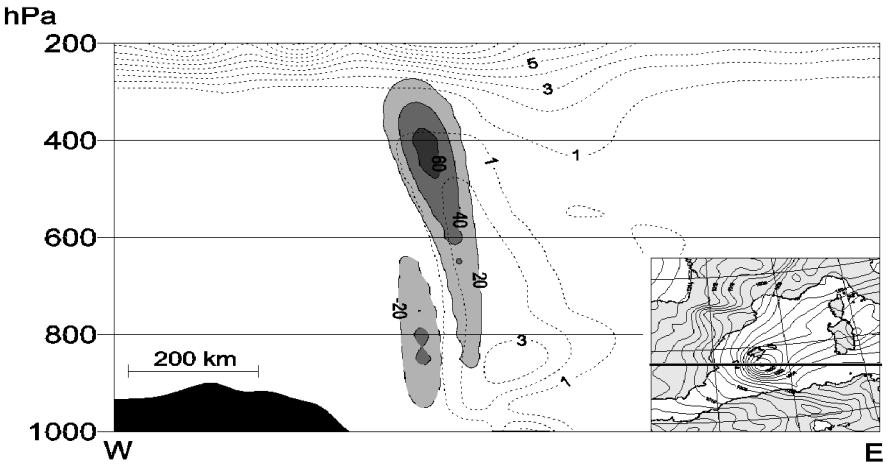

Figure 7. Vertical section across the surface cyclone centre (thick line in the insert map), showing potential vorticity (PV units, dashed line) and vertical velocity (cm s^{-1}, shaded) at 1200 UTC 12 September 1996.

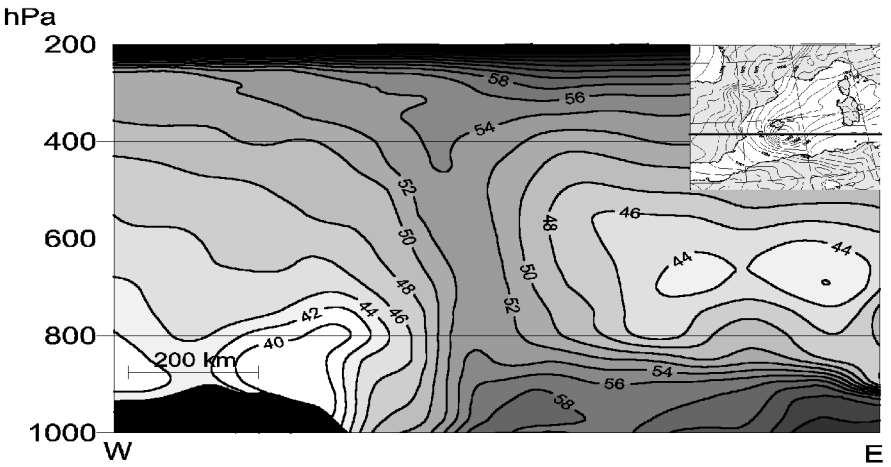

Figure 8. Vertical section across the surface cyclone centre (thick line in the insert map), showing equivalent potential temperature (°C) at 1200 UTC 12 September 1996.

except those derived from features introduced through the initial and boundary conditions. The simulations with no latent-heat flux (hereafter, EXP01) and no sensible-heat flux (hereafter, EXPNSHF) eliminate the latent- and sensible-heat fluxes, respectively, only over the sea in the Hong and Pan (1996) planetary boundary-layer parametrization. Lastly, the dynamical forcing associated with the upper-level trough is reduced during the simulation by appropriately modifying the model initial conditions. In particular, the vorticity and temperature structures linked to the PV disturbance are smoothed out in the initial conditions, and it is assumed that this results in a reduction of the forcing throughout the simulation.

When manipulating dynamical structures, the mass and wind field balances must be preserved to avoid spurious influences on the model integration. Consequently, the

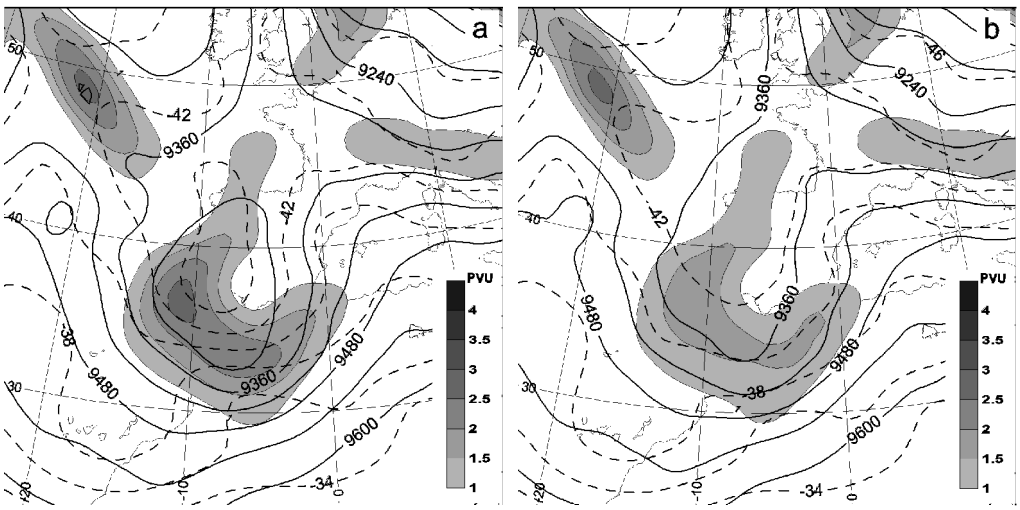

Figure 9. Initial conditions of geopotential height (gpm, full lines) and temperature (°C, dashed lines) for (a) EXP11 and (b) EXP10 (see text) at 300 hPa. Shaded areas represent the potential-vorticity field (PV units) at 300 hPa, also at 1200 UTC 11 September 1996.

PV field is used to select the structure of interest, and the PV-inversion technique of Davis and Emanuel (1991) is applied to determine a balanced flow associated with this feature. This combined mass and wind structure can be used to alter consistently the initial state. The PV anomaly that characterizes the mid-to-upper tropospheric trough is obtained by defining a perturbation PV field, calculated as the departure from the horizontal mean at each isobaric level across the outer grid domain. The anomaly shape is specified manually as the volume that encompasses the cut-off low. The anomaly intensity is calculated to avoid discontinuities in the remaining PV field at the boundary of the PV anomaly. The basic state PV field is equal to the total PV field except at the points corresponding to the PV anomaly. For these points, the basic state PV is set equal to a constant value for each isobaric level equal to the value of the total PV field at the anomaly boundary (e.g. 1.35 PVU at 300 hPa). The anomaly intensity is obtained by subtracting the basic field from the total PV field. Finally, the inverted balanced fields from the PV anomaly are subtracted from the EXP11 initial conditions, obtaining the initial conditions for EXP10.

The elimination of the PV anomaly from the model initial conditions results in a modification at all atmospheric levels, particularly about the Iberian Peninsula. At upper levels, where modifications are most substantial, a distinct trough still remains in the modified initial conditions of EXP10 (Fig. 9). This is due to the definition of the PV anomaly, which was chosen not to change the synoptic pattern drastically (e.g. completely eliminate the trough), but only to diminish the intensity of certain features that appear to be significant for the low-level cyclogenesis, such as the vorticity centre and temperature gradients.

A comparison of the sea-level pressure and the total accumulated precipitation at 1200 UTC 12 September among the five sensitivity experiments and the control run is conducted (Fig. 10). The results from EXPNORO (Fig. 10(b)) show a very similar sea-level pattern to that of EXP11 except for the lack of mesoscale structures near the mountain ranges, such as the Pyrenees and Atlas mountains (see Fig. 1). However,

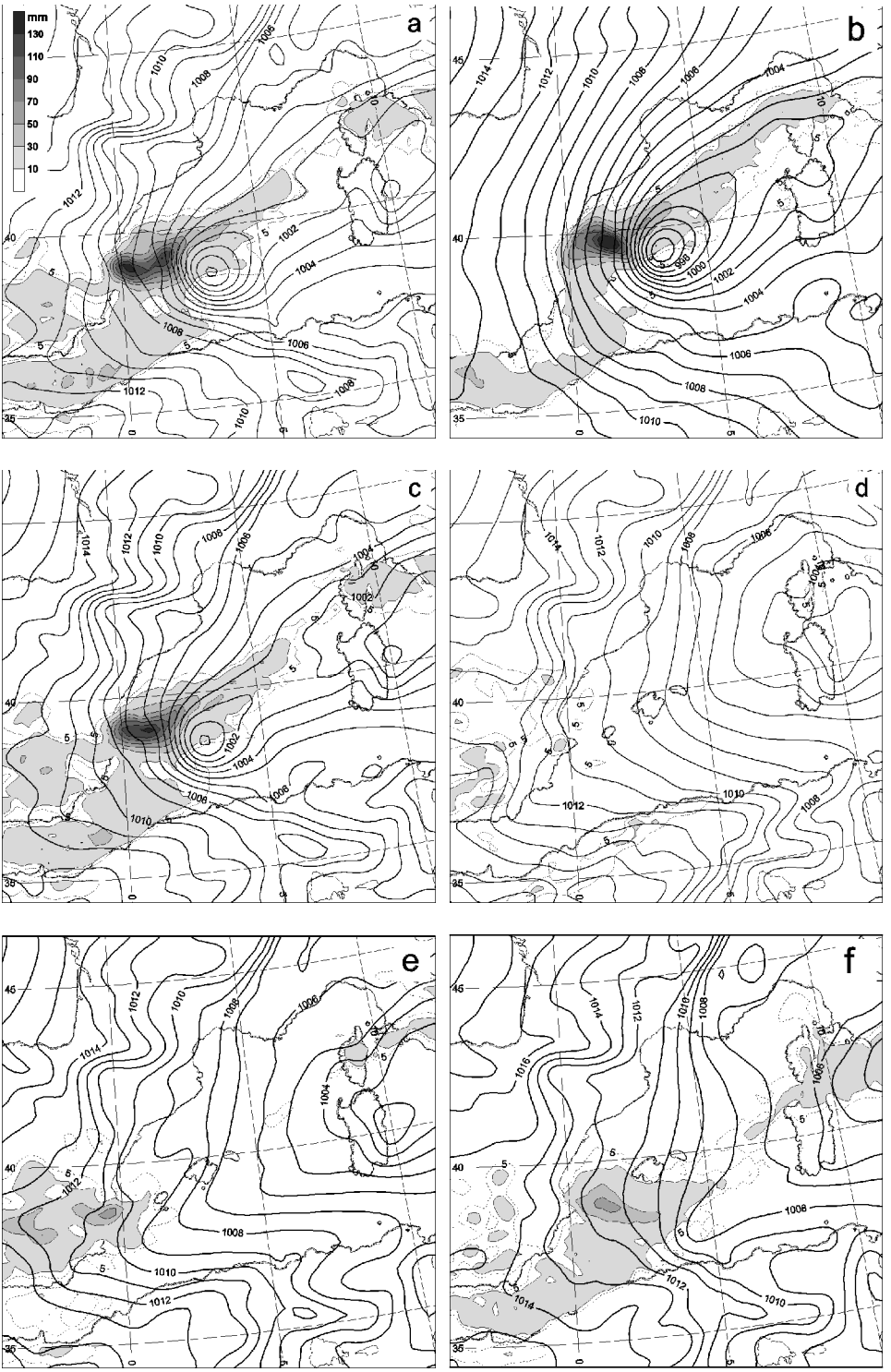

Figure 10. Sea-level pressure (hPa, full lines) and accumulated precipitation (mm, shaded) at 1200 UTC 12 September 1996 for (a) EXP11, (b) EXPNORO, (c) EXPNSHF, (d) EXPNLHR, (e) EXP01 and (f) EXP10 (see text). The dotted line depicts the 5 mm isohyet.

the minimum cyclone sea-level pressure is less in EXPNORO than in the control run. The precipitation distribution obtained from the non-orographic simulation shows an increase in the accumulated precipitation when compared with the control run. Thus, the orography appears to inhibit slightly both the precipitation and the development of the quasi-tropical cyclone. Likewise, the experiment EXPNSHF (Fig. 10(c)) simulates both the small cyclone and a precipitation distribution that are very similar to those in the control run, though a slightly shallower cyclone centre is obtained (2 hPa more at 1200 UTC 12 September). This, unlike other similar events (Pytharoulis *et al.* 1999), reveals that the direct warming from the sea had a weak effect on this cyclone development. In contrast, the results from EXPNLHR (Fig. 10(d)) show a completely different sea-level-pressure distribution from EXP11, since no cyclone is developed by the model. This confirms the crucial role played by the latent-heat release on the development of this event. This also highlights the resemblance of this cyclone development to the cold-low (hurricane-like) polar-low type (Businger and Reed 1989) presented by Billing *et al.* (1983) and Rasmussen and Zick (1987). From the PV point of view, it is clear that the deep PV anomaly observed in Fig. 7 was generated diabatically through latent-heat release. Similarly, notable differences from EXP11 occur in EXP01 and EXP10 (Figs. 10(e) and (f)). These runs do not develop the small cyclone, and the simulated precipitation amounts are much lower than in EXP11. In EXP10 and EXP01, only weak troughs are identified to the south of the Balearics in the sea-level-pressure field. These results indicate the important contribution of both the evaporation from the sea, through the consequent enhanced latent-heat release, and the upper-level disturbance on the genesis of the cyclone and the production of precipitation.

Discussions on whether the baroclinic or the convective mechanism of development is the more relevant in polar-low formation are common in the literature (Businger and Reed 1989). Emanuel and Rotunno (1989) hypothesize that baroclinic instability is a candidate to operate in the early stages of the cyclone formation, as a spin-up mechanism. Then they show that air–sea interaction is able to sustain the cyclone intensity. Their theoretical axisymmetric model of mature hurricanes, which diagnoses the equilibrium central surface pressure of the hurricane from several low and ambient environment parameters, has been used on this Mediterranean cyclone (see Emanuel and Rotunno (1989) for model details). This model assumes that air–sea interaction instability is acting in the system. A minimum sea-level-pressure value of 993 hPa is obtained for the cyclone at 1200 UTC. This value compares quite well with the 992 hPa observed value at Palma de Mallorca (Fig. 2(b)). As already noted by Emanuel and Rotunno (1989), this agreement *suggests but does not entirely prove* that surface fluxes were instrumental in the development of this cyclone.

The factor-separation technique of Stein and Alpert (1993) is used to determine the quantitative effects of evaporation and the upper-level PV anomaly, as well as their interaction, in the cyclone life cycle. Once the important agents acting on a system are identified, this technique allows one to determine unambiguously their joint and mutually independent effects (Alpert *et al.* 1995). This technique requires the realization of 2^n numerical experiments, where n is the number of considered factors. Then, by algebraically combining the model output fields (e.g. precipitation or sea-level pressure), one can isolate the effects due to the individual selected factors and their mutual interactions. In particular, since we have determined the evaporation and the upper-level cut-off low to be governing agents in the cyclone formation, these are the two factors considered in the separation technique. Thus, four experiments are required, designed with the chosen factors adequately turned on and off. If F_{xx} corresponds to any field F obtained from the simulations EXPxx (see Table 1) and E is the effect due to the

latent-heat flux (E_{LHF}), the PV anomaly (E_{PV}), their interaction (E_{INT}) and the non-considered factors (E_{00}), then:

$$\begin{aligned} F_{11} &= E_{\mathrm{LHF}} + E_{\mathrm{PV}} + E_{\mathrm{INT}} + E_{00} \\ F_{10} &= E_{\mathrm{LHF}} + E_{00} \\ F_{01} &= E_{\mathrm{PV}} + E_{00} \\ F_{00} &= E_{00}. \end{aligned}$$

Thus, solving the system to isolate these effects, we obtain:

$$\begin{aligned} E_{\mathrm{LHF}} &= F_{10} - F_{00} \\ E_{\mathrm{PV}} &= F_{01} - F_{00} \\ E_{\mathrm{INT}} &= F_{11} - (F_{10} + F_{01}) + F_{00} \\ E_{00} &= F_{00}. \end{aligned}$$

Figure 11 shows the factor-separation results on the sea-level-pressure field. At 0000 UTC 12 September (Fig. 11(b)) the PV anomaly appears to produce a general deepening of more than 3 hPa over the western Mediterranean, with a small area exceeding 5 hPa offshore the Valencian coast. This focused region of deepening produces an increase in the north-easterly flow towards and within the Balearic channel during the hours before the small-cyclone development. The presence of north-easterly winds over this area has been shown to favour heavy precipitation over the Valencia region (Homar *et al.* 1999; Romero *et al.* 2000). The effects of the PV anomaly are observed to dominate the cyclone evolution during the first 6 hours of 12 September, contributing to about 80% of the total deepening produced by these factors at 0000 UTC, and to about 50% at 0600 UTC 12 September (Fig. 11(a)). Before 0600 UTC, neither the pure latent-heat flux factor nor its interaction with the PV anomaly had a significant effect on the sea-level-pressure field. This reveals the PV anomaly aloft as the triggering mechanism for the air–sea interaction instability, shown as necessary by Emanuel (1986).

At 1200 UTC, well after cyclone formation, a broad negative contribution of 4–5 hPa is obtained from the PV anomaly factor over the area occupied by the synoptic low (Fig. 11(c)). The latent-heat flux factor tends, weakly, to extend the region of lower pressure to the south-east. However, the PV–latent-heat flux interaction exerts an important role on the strength (Fig. 11(a)) and shape (Fig. 11(c)) of the cyclone at this time. It contributes more than 6 hPa, or nearly 50%, of the deepening at the cyclone centre. In contrast with the other factors, the interaction factor influences a very limited horizontal region (Fig. 11(c)) because the convection is very localized over the cyclone. Yet it is the main contributor to the deepening at the centre of the small cyclone. These results indicate that the PV–latent-heat flux interaction factor is the most important agent for the intensification of the quasi-tropical cyclone. The interpretation of this interaction should not be viewed as a simultaneous united action of both factors, but as a resultant collaborative effect, which would not have occurred without both contributions: an initial spin-up of the system mainly forced by the upper-level PV anomaly and a further evaporation from the sea with subsequent diabatic warming at mid levels.

Two additional experiments were performed in order to confirm the interpretation of the interaction-factor effect before the cyclone formation and during its eastward progression. Consider 0600 UTC 12 September as the time of cyclone formation. Experiment EXP01A turns off latent-heat flux after that time, while EXP01B turns off latent-heat flux before that time. Results from EXP01B clearly highlight the critical

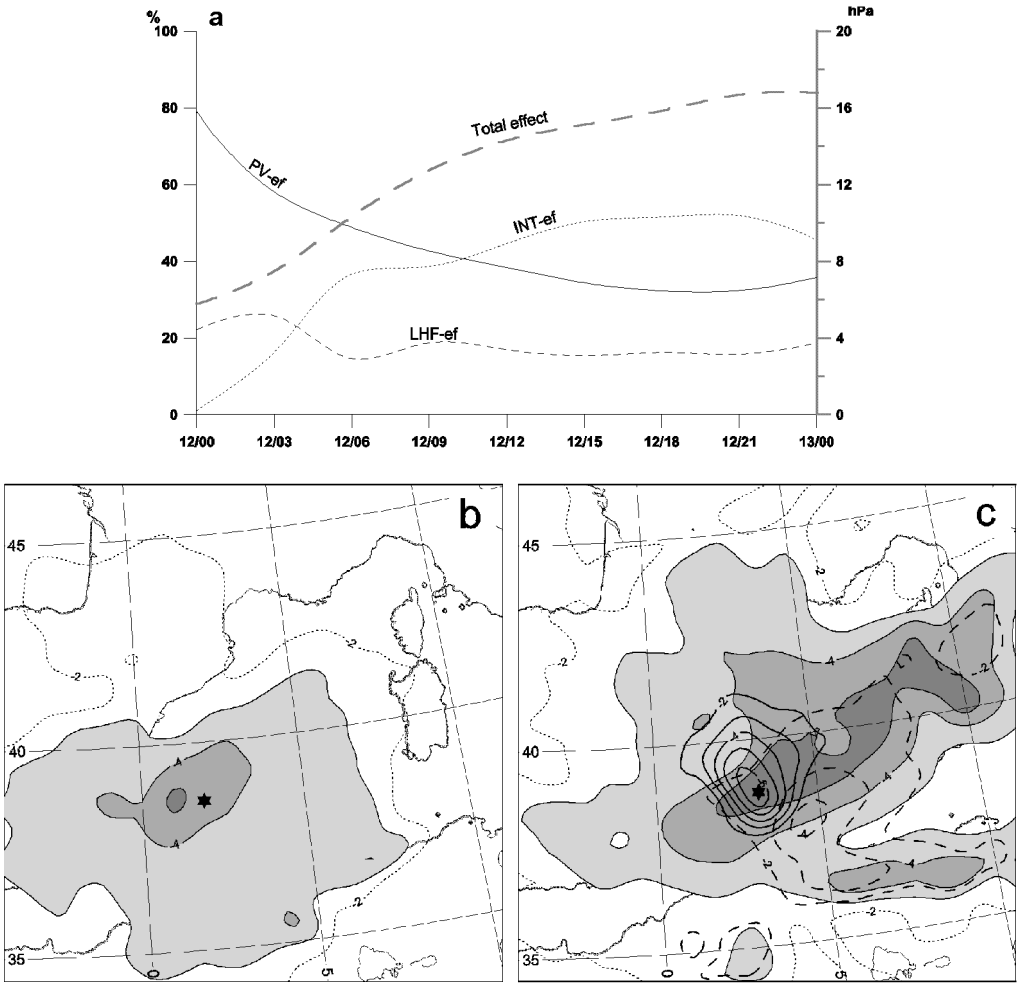

Figure 11. Factor-separation results on the sea-level pressure. (a) The effects of each factor at the cyclone centre (% relative to the total effect attributable to the considered factors) during 12 September 1996. Grey dashed line is scaled on the right axis and corresponds to the absolute value of the total effect due to the considered factors on the cyclone deepening. Spatial distribution of the effects of the potential-vorticity (PV) anomaly (shaded, dotted line represents −2 hPa), the latent-heat flux (LHF, dashed lines) and the interaction (INT, full lines) at (b) 0000 UTC and (c) 1200 UTC 12 September 1996. Stars represent the cyclone centre location in the control simulation.

role of latent-heat flux before cyclone formation, since no cyclone is obtained in this simulation. Even when latent-heat flux is activated at 0600 UTC, there is not enough moisture at low levels to develop convection and diabatically heat the mid-level atmosphere. On the other hand, EXP01A points out the role of the latent-heat flux during the mature stage of the cyclone, which helps to feed the convective systems with moisture-rich air and thus maintains the diabatic heat source for continued cyclone deepening (Fig. 12).

The factor-separation technique also has been applied to the 3-hour accumulated precipitation field. The influences of the individual factors on this parameter are negligible for all the simulations, but the effect due to synergisms is large. At 0600 UTC 12 September a rainfall region of more than 65 mm in 3 h is seen offshore the Valencian coast (Fig. 13). The presence of a weak negative contribution near the positive nucleus

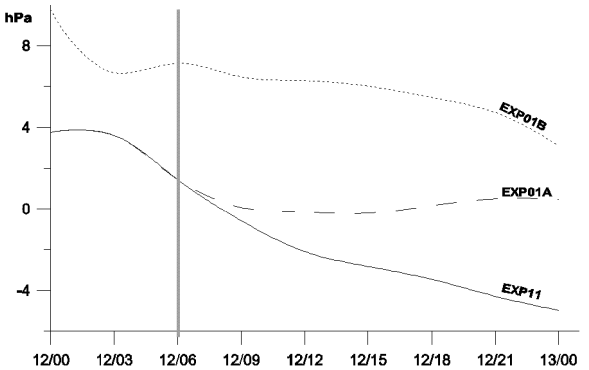

Figure 12. Evolution of the cyclone central sea-level pressure (hPa) during 12 September 1996. Full line depicts EXP11, dashed line depicts EXP01A and dotted line depicts EXP01B results. Vertical mark at 0600 UTC represents the time at which the latent-heat flux parametrization is switched off for EXP01A and switched on for EXP01B (see text for details).

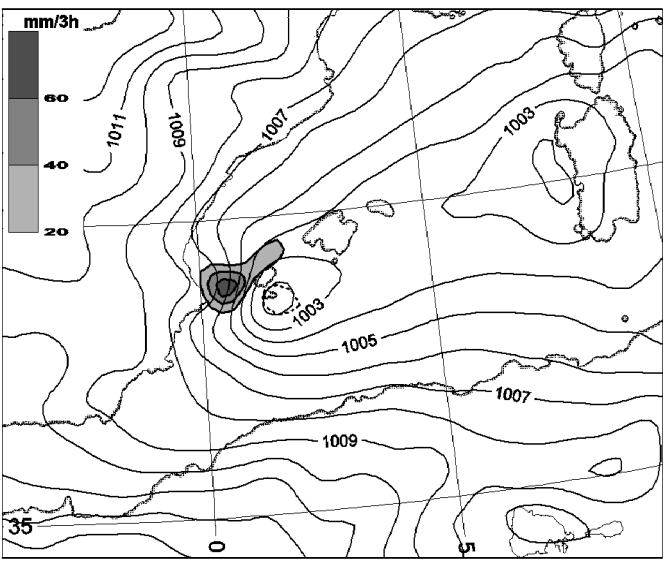

Figure 13. Effect on the 3 h accumulated precipitation (mm per 3 h) of the latent-heat flux–potential vorticity interaction factor. Only absolute values larger than 20 mm per 3 h are depicted. Shaded areas indicate positive values and dashed lines negative. Sea-level pressure (hPa) from EXP11 (see text) at 0600 UTC 12 September 1996 is depicted with full lines.

over the sea is due to focusing the precipitation near the Valencia coast at the expense of precipitation in the adjacent oceanic areas. The strong and focused positive precipitation signature indicates the important influence of both the upper PV anomaly and the latent-heat flux when acting together for convective development. A vertical cross-section of the contribution to the vertical velocity and divergence fields by the interaction factor shows a clear signature of deep convection over the western Mediterranean (Fig. 14). This important role played by the evaporation suggests, but does not strictly prove, that air–sea instability was instrumental in the development of this cyclone.

Furthermore, a study on the sensitivity of the sea-level pressure, and the cyclone formation in particular, to the SST was done. Experiments using a 2 and 5 degC cooler

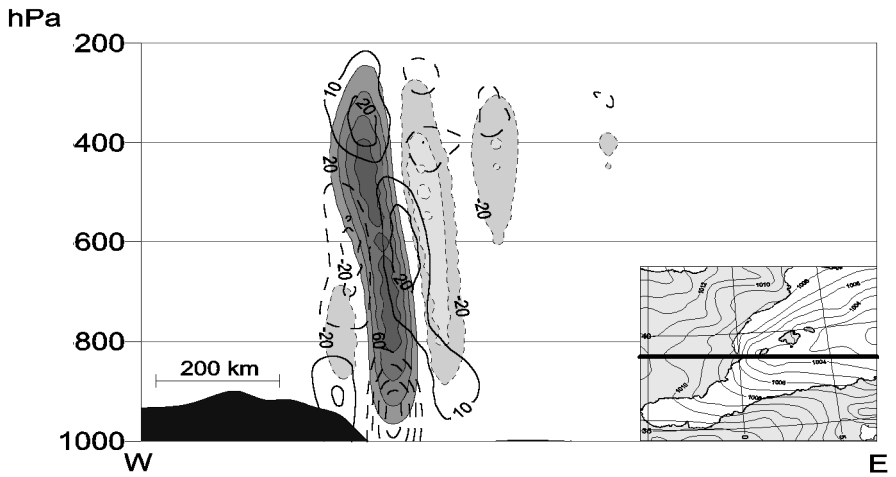

Figure 14. Vertical cross-section along the thick line on the insert map showing the effect on the vertical velocity (cm s^{-1}, shaded) and horizontal wind divergence (s^{-1}, unshaded contours) of the latent-heat flux–potential vorticity interaction factor at 0300 UTC 12 September 1996. Positive values are plotted with full lines and negative values with dashed lines.

sea surface were performed. No experiments with warmer SSTs were considered since the key role of the evaporation on the development of the cyclone has been already highlighted without any artificial SST warming. Figure 15 shows a comparison among the sea-level pressure at 1200 UTC and the latent-heat flux at 0000 UTC 12 September obtained from the cooled-SST experiments and EXP11. The 2 degC-cooled-sea experiment (Fig. 15(b)) simulates the cyclone, but it is weaker and with a delay with respect to EXP11 (Fig. 15(a)). This delay and the cyclone weakening is even greater in the 5 degC-cooled-sea experiment (Fig. 15(c)), which does not simulate the cyclone due to the slower moistening of the lower layers and the consequent delay of the convective triggering as consequence of the absence of convective instability in the early hours of the run. This reveals the importance of a warm sea for this case, which was necessary to produce intense evaporation, together with the upper-level PV anomaly forcing, to trigger the convection which initiated the former evolution. In addition, Fig. 15(b) shows that, although enough evaporation to achieve closed circulation could exist for SST 2 degC cooler than the control run, weaker evaporation results from the cyclonic flow and so deepening is not as intense as in the EXP11 run.

In summary, the previous factor-separation study suggests that the intense, small-scale cyclogenesis event occurred according to the following scenario: before the genesis of the cyclone, the upper-level PV anomaly intensified the synoptic low and therefore enhanced the north-easterly surface winds over the Balearic channel. This wind enhancement contributed to a notable increase in the latent-heat flux from the sea (Fig. 16). Thus, the mesoscale features of the low-level flow due to the upper-level PV anomaly not only favoured the triggering of convection by creating convergent areas offshore Valencia, but also contributed to the convective destabilization of the lower troposphere through increased latent-heat flux from the sea. Once a favourable environment was produced, and convection developed, the latent heat released from convection further induced cyclogenesis through diabatic heating over a deep column. This enhanced the cyclone intensity and the associated surface winds, leading to greater latent-heat flux, and resulting in a hurricane-like energy engine via air–sea interaction instability.

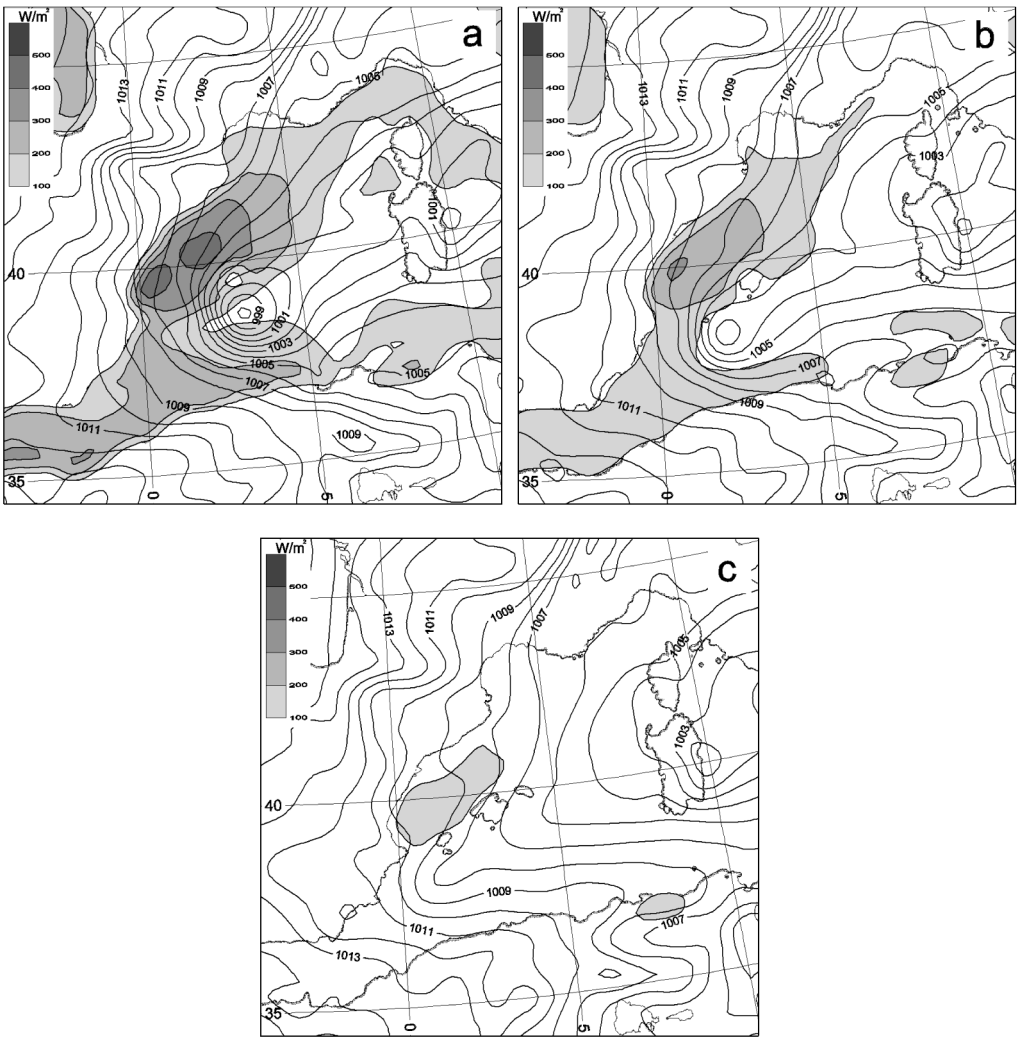

Figure 15. Sea-level pressure (hPa, full lines) at 1200 UTC and latent-heat flux (W m^{-2}, shaded) at 0000 UTC 12 September 1996 for (a) EXP11, (b) 2 degC cooled sea surface temperature (SST), and (c) 5 degC cooled SST relative to EXP11 (see text).

4. CONCLUSIONS

The mechanisms leading to the genesis of a small, quasi-tropical cyclone observed on 12 September 1996 over the western Mediterranean have been investigated. Some features observed in common with certain polar lows, small cyclones that usually develop at high latitudes (Businger and Reed 1989), have been described. Numerical experiments were performed to examine the role of several factors which were identified as important to this event in previous studies. The control run produces intense evaporation from the sea and deep convection before cyclone formation, suggesting that diabatic heating from condensation is a key mechanism for cyclogenesis. A numerical sensitivity analysis confirmed the primary role of the latent-heat release on the cyclogenesis, and further revealed that orography played almost no role in this event. Although the impinging of the low-level flow on the orography is usually a triggering mechanism

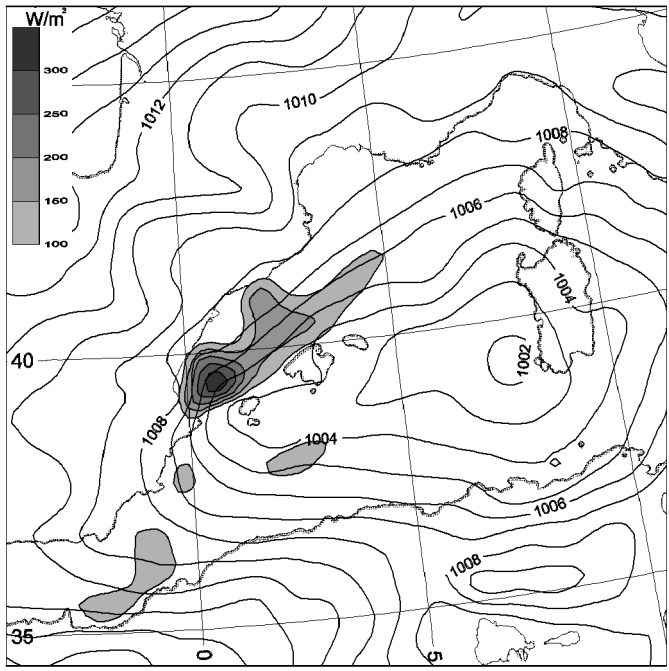

Figure 16. Latent-heat flux (W m^{-2}, shaded) owing to the potential-vorticity anomaly influence at 0300 UTC 12 September 1996. Full lines represent sea-level pressure (hPa) at the same time for EXP11 (see text).

for convection in the area, it did not substantially influence the convective development on this day. Unlike other studies of similar Mediterranean small-scale cyclones, experiments reveal that the sensible-heat flux from the sea played only a secondary role on the precipitation production and the further sea-level-pressure deepening. Instead, using a factor-separation technique, the intensity of the upper-level cut-off low and the latent-heat flux from the sea emerged as crucial factors for the quasi-tropical cyclogenesis. These conclusions were aided by the application of a PV-inversion technique that led to a decrease of the intensity of the synoptic mid- and upper-level cut-off low, while preserving the dynamical and thermodynamic balance of the meteorological fields.

The effect of the upper-level disturbance on the sea-level pressure is shown to act principally on the scale of the synoptic surface low sited over the western Mediterranean basin. The small-scale cyclone deepening is mainly attributable to the interaction between this PV anomaly and the latent-heat flux from the sea. However, early in the cyclone development, the enhanced surface circulation due to the upper-level anomaly enhanced the north-easterly warm advection within the Balearic channel. This increased the evaporation from the sea that was essential for the triggering of deep convection. This process resembles an air–sea interaction instability, since the initial convective activity is sustained by strong latent-heat fluxes, which are enhanced by the low-level circulation forced by the diabatic heating from convection.

This small-scale cyclogenesis is, to some extent, an example of a polar-low-like development in which the convective activity is essential, in contrast to baroclinic development. The role of the upper-level PV structures in the present case has not been found to act directly on the cyclone deepening, but indirectly through an enhancement of the surface circulation, favouring the starting-up of the air–sea interaction instability.

Thus, both a strengthening of the surface flow by the upper-level trough and a moistening of the low levels by evaporation from the sea were necessary for the development of the small-scale cyclone.

Results from a theoretical axisymmetric model of hurricanes (Emanuel and Rotunno 1989) suggests that air–sea interaction is able to sustain the observed cyclone intensity. In addition, a numerical experiment, in which the surface evaporation is neglected until after the strengthening of the surface flow by the upper-level trough has evolved eastwards, shows that the cyclone does not develop. In contrast, a numerical experiment in which the evaporation is neglected after the cyclone develops shows that the cyclone does not deepen further, and actually fills slightly. These results are consistent with those of Bresch *et al.* (1997) in a study of a polar low over the Bering Sea.

These results highlight the importance of an adequate estimation of the intensity and shape of the upper-level flow structures in the analyses ingested by numerical models, since the forecasts of small-scale features are extremely sensitive to these flow structures. In addition, accurate observations of sea surface temperature and low-level circulations are crucial to improve the forecasts of severe weather over the western Mediterranean basin.

ACKNOWLEDGEMENTS

This research was mainly developed while the lead and second authors were on an extended visit to the National Severe Storms Laboratory (NSSL). The authors thank the helpful suggestions made by Dr D. Schultz. Pressure and precipitation data were provided by the Instituto Nacional de Meteorología (INM) of Spain. Computer support provided by NCAR/Scientific Computer Division (which is sponsored by the National Science Foundation) for model data preprocessing is also acknowledged. We wish to thank the reviewers for their suggestions, which helped to improve the study and clarify the text. This work has been partially supported by the CICYT CLI99-0269 and REN 2002-03482 grants.

REFERENCES

Alpert, P., Neeman, B. U. and Shay-El, Y. 1990 Climatological analysis of Mediterranean cyclones using ECMWF data. *Tellus*, **42A,** 67–77

Alpert, P., Tsidulko, M. and Stein, U. 1995 Can sensitivity studies yield absolute comparisons for effects of several processes? *J. Atmos. Sci.*, **52,** 597–601

Alpert, P., Tzidulko, M. and Izigsohn, D. 1999 A shallow short-lived meso-beta cyclone over the gulf of Antalya, eastern Mediterranean. *Tellus.*, **51A,** 249–262

Benjamin, S. B. and Seaman, N. L. 1985 A simple scheme for improved objective analysis in curved flow. *Mon. Weather Rev.*, **113,** 1184–1198

Billing, H., Haupt, I. and Tonn, W. 1983 Evolution of a hurricane-like cyclone in the Mediterranean Sea. *Beitr. Phys. Atmos.*, **56,** 508–510

Bleck, R. 1990 Depiction of upper/lower vortex interaction associated with extratropical cyclogenesis. *Mon. Weather Rev.*, **118,** 573–585

Bresch, J. F., Reed, R. J. and Albright, M. D. 1997 A polar-low development over the Bering Sea: Analysis, numerical simulation, and sensitivity experiments. *Mon. Weather Rev.*, **125,** 3109–3130

Businger, S. and Reed, R. J. 1989 Cyclogenesis in cold air masses. *Weather and Forecasting*, **4,** 133–156.

Campins, J., Genovés, A., Jansà, A., Guijarro, J. A. and Ramis, C. 2000 A catalogue and a classification of surface cyclones for the western Mediterranean. *Int. J. Climatol.*, **20,** 969–984

Davis, C. A. and Emanuel, K. 1991 Potential vorticity diagnostics of cyclogenesis. *Mon. Weather Rev.*, **119,** 1929–1953

Doswell III, C. A., Ramis, C., Romero, R. and Alonso, S. 1998 A diagnostic study of three heavy precipitation episodes in the western Mediterranean. *Weather and Forecasting*, **13,** 102–124

Dudhia, J. 1993 A nonhydrostatic version of the Penn State/NCAR mesoscale model: Validation tests and simulation of an Atlantic cyclone and cold front. *Mon. Weather Rev.*, **121,** 1493–1513

Emanuel, K. A. 1986 An air–sea interaction theory for tropical cyclones. Part I: Steady-state maintenance. *J. Atmos. Sci.*, **43,** 585–604

Emanuel, K. A. and Rotunno, R. 1989 Polar lows as arctic hurricanes. *Tellus A*, **41,** 1–17

Ernst, J. A. and Matson, M. 1983 A Mediterranean tropical storm? *Weather*, **38,** 332–337

Grell, G. A., Dudhia, J. and Stauffer, D. R. 1995 'A description of the fifth-generation Penn State/NCAR mesoscale model (MM5)'. NCAR Tech. Note NCAR/TN-398+STR

Homar, V., Ramis, C., Romero, R., Alonso, S., García-Moya, J. and Alarcón, M. 1999 A case of convection development over the western Mediterranean Sea: A study through numerical simulations. *Meteorol. Atmos. Phys.*, **71,** 169–188

Homar, V., Gayà, M. and Ramis, C. 2001 A synoptic and mesoscale diagnosis of a tornado outbreak in the Balearic Islands. *Atmos. Res.*, **56,** 31–55

Hong, S. Y. and Pan, H. L. 1996 Nonlocal boundary layer vertical diffusion in a medium-range forecast model. *Mon. Weather Rev.*, **124,** 2322–2339

Huo, Z., Zhang, D.-L. and Gyakum, J. R. 1999 Interaction of potential vorticity anomalies in extratropical cyclogenesis. Part I: Static piecewise inversion. *Mon. Weather Rev.*, **127,** 2546–2561

Kain, J. S. and Fritsch, J. M. 1990 A one-dimensional entraining/detraining plume model and its application in convective parameterization. *J. Atmos. Sci.*, **47,** 2784–2802

1997 Multiscale convective overturning in mesoscale convective systems: Reconciling observations, simulations and theory. *Mon. Weather Rev.*, **126,** 2254–2273

Lin, Y. L., Farley, R. D. and Orville, H. D. 1983 Bulk parameterization of the snow field in a cloud model. *J. Clim. Appl. Meteorol.*, **22,** 1065–1092

Pagowski, M. and Moore, G. W. K. 2001 A numerical study of an extreme cold-air outbreak over the Labrador Sea: Sea ice, air–sea interaction, and development of polar lows. *Mon. Weather Rev.*, **129,** 47–72

Petterssen, S. 1956 *Weather analysis and forecasting* (vol. 1). McGraw-Hill Company, New York, USA

Pytharoulis, L., Craig, G. C. and Ballard, S. P. 1999 Study of the hurricane-like Mediterranean cyclone of January 1995. *Phys. Chem. Earth (B)*, **24,** 627–632

Ramis, C., Romero, R., Homar, V., Alonso, S. and Alarcón, M. 1998 Diagnosis and numerical simulation of a torrential precipitation event in Catalonia (Spain). *Meteorol. Atmos. Phys.*, **69,** 1–21

Rasmussen, E. 1985 A case study of a polar low development over the Barents Sea. *Tellus A*, **37,** 407–418

Rasmussen, E. and Zick, C. 1987 A subsynoptic vortex over the Mediterranean Sea with some resemblance to polar lows. *Tellus*, **39,** 408–425

Reale, O. and Atlas, R. 2001 Tropical cyclone-like vortices in the extratropics: Observational evidence and synoptic analysis. *Weather and Forecasting*, **16,** 7–34

Romero, R., Ramis, C. and Alonso, S. 1997 Numerical simulation of an extreme rainfall event in Catalonia: Role of orography and evaporation from the sea. *Q. J. R. Meteorol. Soc.*, **123,** 537–559

Romero, R., Doswell III, C. A. and Ramis, C. 2000 Mesoscale numerical study of two cases of long-lived quasi-stationary convective systems over eastern Spain. *Mon. Weather. Rev.*, **128,** 3731–3751

Staley, D. O. and Gall, R. L. 1977 On the wavelength of warm baroclinic instability. *J. Atmos. Sci.*, **34,** 1679–1688

Stein, U. and Alpert, P. 1993 Factor separation in numerical simulations. *J. Atmos. Sci.*, **50,** 2107–2115

Tao, W. and Simpson, J. 1993 Goddard cumulus ensemble model. Part I: Model description. *Terrestr. Atmos. Ocean. Sci.*, **4,** 35–72

Tsidulko, M. and Alpert, P. 2001 Synergism of upper-level potential vorticity and mountains in Genoa lee cyclogenesis: A numerical study. *Meteorol. Atmos. Phys.*, **78,** 261–285

Tudurí, E. and Ramis, C. 1997 The environments of significant convective events in the western Mediterranean. *Weather and Forecasting*, **12,** 294–306